Atmos. Chem. Phys. Discuss.,
https://doi.org/10.5194/acp-2018-935-AC1, 2019

Atmospheric Chemistry and Physics Discussions

Interactive comment on "Oligomerization Reactions of Criegee Intermediates with Hydroxyalkyl Hydroperoxides: Mechanism, Kinetics, and Structure-Reactivity Relationship" *by* Long Chen et al.

Long Chen et al.

huangyu@ieecas.cn

Received and published: 31 January 2019

Prof. Yu Huang Key Lab of Aerosol Chemistry & Physics, Institute of Earth Environment, Chinese Academy of Sciences, Xi'an, 710061, China Tel./Fax: (86) 29-62336261 E-mail: huangyu@ieecas.cn Jan. 31, 2019 Dear reviewer, Revision for Manuscript acp-2018-935 We thank you very much for giving us the opportunity to revise our manuscript. We highly appreciate the reviewer for their comments and suggestions on the manuscript entitled "Mechanistic and Kinetics Investigations of Oligomer Formation from Criegee Intermediates Reactions with Hydroxyalkyl Hydroperoxides". We

have made revisions of our manuscript carefully according to the comments and suggestions of reviewer. The revised contents are marked in blue color. The response letter to reviewers is attached at the end of this cover letter. We hope that the revised manuscript can meet the requirement of Atmospheric Chemistry & Physics. Any further modifications or revisions, please do not hesitate to contact us. Look forward to hearing from you as soon as possible.

Best regards, Yu Huang âĂČ Comments of reviewer #1 1. The sentence on lines 45-48 is plagiarized from Donahue et al.(1) I do not have the resources to fully vet the rest of this manuscript, but all text must be in your own words. You cannot copy such ïňĄne sentences as if they were your own. ALL instances of copied text must be removed and replaced with text you produce. Response: We are sorry for this. The original sentence in the revised manuscript is "Alkene ozonolysis produces a carbonyl oxide (also called Criegee intermediates (CIs)) and a carbonyl moiety". Corresponding descriptions have been revised in the page 3 line 43-46 of the revised manuscript: Alkene ozonolysis produces a carbonyl oxide (also called Criegee intermediates (CIs)) and a carbonyl moiety (Donahue et al., 2011; Aplincourt et al., 2000; Johnson et al., 2008; Welz et al., 2012; Criegee et al., 1975; Taatjes et al., 2013). Moreover, all text in the revised manuscript has been checked carefully using our own words. 2. Please make clear throughout that the reactions studied are minor loss processes for CI. Your lifetime of 6000 seconds is quite long compared to other CI reactions. In addition, make explicitly clear that you calculate the lifetime with respect to only reaction with HHP. You often speak of just "lifetime" and do not specify reaction with HHP. Response: Previous experimental and theoretical investigations have shown that unimolecular decay of CI and its reaction with water are the dominant chemical sinks (Smith, et al., 2015; Taatjes, et al., 2013; Chao et al., 2015; Anglada, et al., 2016; Long et al., 2016, 2018, Lester et al., 2018). The main products of CIs reactions with water are hydroxyalkyl hydroperoxides (HHPs), which are important sources of hydroperoxides and carbonyl compounds (Anglada, et al., 2016; Kumar, et al., 2014). Although the carbonyl oxides reactions with HHPs are minor loss processes, the type of reactions is very important for under-

standing the first step of new particle formation form alkenes ozonolysis, particularly in heavily forested area. Our results demonstrate that the oligomer formations from CIs reactions with HHPs are both thermochemically and kinetically favoured. As shown in Table 2, the room temperature rate coefficient kR9 is 1.5 $\times$ 10-9 cm3 molecule-1 s-1. Assuming that the concentration of HO-CH2OO-H (Pa1) is approximately equal to that of SCIs ($\sim$ 5.0 $\times$ 104 moleculesâĂćcm-3, within an order of magnitude uncertainty) in the boreal forest and rural environments of Finland and Germany (Novelli et al., 2016, 2017). The fate τ can be written as eqn (1) (Long et al., 2016): (1) where k and [X] represent the rate coefficient and the reactant concentration. The atmospheric lifetime of anti-CH3CHOO reactivity toward Pa1 is 1.3-13 $\times$ 103 s. The experimental rate coefficient of anti-CH3CHOO reaction with water dimer approximately equals $\sim$ 1.0 $\times$ 10-11 cm3 molecule-1 s-1 at 298 K (Lin, et al., 2016). The concentration of water dimer is 5.5 $\times$ 1013 moleculesâĂćcm-3 at 3 km altitude (Long et al., 2016). The atmospheric lifetime of anti-CH3CHOO reactivity toward water dimer is 1.8 $\times$ 10-3 s. The result implies that the reactions studied are minor loss processes in the atmosphere. However, the [(H2O)2] decreases significantly with increasing altitudes. For example, at 15 km altitude, the [(H2O)2] is 2.7 $\times$ 106 molecules cm-3 (Long et al., 2016), the atmospheric lifetime of anti-CH3CHOO is 3.4 $\times$ 104 s. As discussed above, it can be found that the anti-CH3CHOO + Pa1 reaction can compete with the anti-CH3CHOO + (H2O)2 reaction in some regions where the altitude is above 15 km. Corresponding descriptions have been added in the page 20 line 549-564 of the revised manuscript: The room temperature rate coefficient kR9 is 1.5 $\times$ 10-9 cm3 molecule-1 s-1. Assuming that the concentration of Pa1 is approximately equal to that of SCIs ($\sim$5.0 $\times$ 104 moleculesâĂćcm-3, within an order of magnitude uncertainty) in the boreal forest and rural environments of Finland and Germany (Novelli et al., 2016; 2017). The atmospheric lifetime of anti-CH3CHOO reactivity toward Pa1 can be estimated as 1.3-13 $\times$ 103 s. The experimental rate coefficient of reaction R12 approximately equals $\sim$ 1.0 $\times$ 10-11 cm3 molecule-1 s-1 at 298 K (Lin et al., 2016). The concentration of water dimer is 5.5 $\times$ 1013 moleculesâĂćcm-3 at 3 km altitude (Long et al., 2016). The atmospheric

lifetime of anti-CH3CHOO reactivity toward water dimer is 1.8 $\times$ 10-3 s. The result implies that the reactions studied are minor loss processes in the atmosphere. However, the [(H2O)2] decreases significantly with increasing altitudes(Long et al., 2016). For example, at 15 km altitude, the [(H2O)2] is 2.7 $\times$ 106 molecules cm-3, the atmospheric lifetime of anti-CH3CHOO is 3.4 $\times$ 104 s. As discussed above, it can be found that the anti-CH3CHOO + Pa1 reaction can compete with the anti-CH3CHOO + (H2O)2 system in some regions where the altitude is above 15 km. 3. The products formed may be subject to other loss processes than thermal unimolecular decay, such as photolysis and reaction with more abundant reaction partners (e.g. OH). The authors need to place the chemistry studied here in a broader context and discuss (even if brieïňĆy) other loss processes. Response: Based on the Reviewer's suggestion, the bimolecular reaction of HO-CH2OO-H(Pa1) with OH radical is investigated at the M06-2X/def2-TZVP//M06-2X/6-311+ G(2df,2p) level of theory, and the corresponding potential energy surface is shown in Figure S5. As seen from Figure S5, the hydrogen abstraction reactions between OH and Pa1 are strongly exothermic and spontaneous, indicating that the occurrence of these reactions in the atmosphere is thermochemically feasible. One can notice that the exothermic reaction RHγ releasing energy is significantly higher than that of the RHα and RHβ. The pre-reactive complexes (IMαH-a, βH-a, and γH-a) are formed in the entrance channel, and followed by proceed the direct hydrogen abstraction processes leading to the products PHα, PHβ, and PHγ plus H2O. The free-energy (ΔGa#) barriers predict TSHα, TSHβ and TSHγ to lie 6.8, 4.8, and 4.4 kcalâĂćmol-1 above the energies of the corresponding pre-reactive complexes IMαH-a, βH-a, and γH-a. The result again shows that the OH abstraction Hγ atom reaction is the most energetically favorable channel. As shown in Figure 2, the addition reactions of 2CH2OO + Pa1 begin with the formation of loosely bound pre-reactive complexes IM1a and IM1b, of 3.1 and 2.6 kcalâĂćmol-1 stability. They are formed by a hydrogen bond between the terminal CH2OO oxygen atom and the hydrogen atom of the -OOH group in Pa1, and a van der Waals (vdW) bond between the central carbon atom of CH2OO and the oxygen atom of the -OH group in Pa1. The above complexes

are immediately converted into products P1a and P1b via transition states TS1a and TS1b with barriers of 8.4 and 11.7 kcalâĂćmol-1, respectively, while the corresponding reaction exothermicities are estimated as 43.4 and 40.5 kcalâĂćmol-1, respectively. The above result shows that the most favorable channel is the addition of the -OOH group of Pa1 to the parent carbonyl oxide. However, the barrier is higher than that of the corresponding hydrogen abstraction reaction RHγ 4.0 kcalâĂćmol-1, indicating that the photochemical oxidation of hydroxyalkyl hydroperoxides is important in the atmosphere. In the present study, we mainly focus on the gas phase reaction mechanism and kinetics of oligomer formation from carbonyl oxides reactions with hydroxyalkyl hydroperoxides. This is because the type of reaction studied is very important for understanding the first step of new particle formation form alkenes ozonolysis, particularly in heavily forested area. Corresponding descriptions have been added in the page 13 line 339-357 of the revised manuscript: Moreover, the bimolecular reaction of Pa1 with OH radical is investigated at the M06-2X/def2-TZVP//M06-2X/6-311+G(2df,2p) level of theory, and the corresponding PES is shown in Figure S5. As seen from Figure S5, the hydrogen abstraction reactions between OH and Pa1 are strongly exothermic and spontaneous, indicating that the occurrence of these reactions in the atmosphere is thermochemically feasible. One can notice that the exothermic reaction RHγ releasing energy is significantly higher than that of the RHα and RHβ. The pre-reactive complexes (IMαH-a, βH-a, and γH-a) are formed in the entrance channel, and followed by proceed the direct hydrogen abstraction processes leading to the products PHα, PHβ, and PHγ plus H2O. The barriers predict TSHα, TSHβ and TSHγ to lie 6.8, 4.8, and 4.4 kcalâĂćmol-1 above the energies of the corresponding pre-reactive complexes IMαH-a, βH-a, and γH-a. The result again shows that the reaction RHγ is the most energetically favorable channel. One can notice that the barrier of RHγ is lower than that of the corresponding addition reaction R1a 4.0 kcalâĂćmol-1, indicating that the photochemical oxidation of HHPs is important in the atmosphere. In the present study, we mainly focus on the gas phase reaction mechanism and kinetics of oligomer formation from carbonyl oxides reactions with HHPs. This is because the type of reaction

studied is very important for understanding the first step of new particle formation form alkenes ozonolysis, particularly in heavily forested area.

Figure S5. PES (ΔG and ΔE (italic)) for the reaction of HO-CH2OO-H (Pa1) with OH computed at the M06-2X/def2-TZVP//M06-2X/6-311+G(2df,2p) level of theory 4. As the major importance of this work relates to formation of secondary organic aerosol, the authors should make a better attempt to compare the possible inïňĆuence of this speciïňĄc chemistry on SOA formation and observed SOA formation from ozonolysis experiments, such as that in Ehn et al.(2) Further it should be clearly stated early on in the manuscript that the reactions studied are gas phase. A reaction with HHP might suggest to many that this chemistry occurs within the particle phase where HHP could have a higher concentration. Response: In the present study, we mainly focus on the gas phase reaction mechanism and kinetics of oligomer formation from carbonyl oxides reactions with HHPs. Our results demonstrate that the consecutive reactions of CIs with HHPs are both thermochemically and kinetically favoured, and the oligomers containing CIs as chain units. Ehn et al. (2014) reported a large source of low-volatility SOA generated from the ozonolysis of α-pinene and other endocyclic monoterpenes under atmospheric conditions, and proposed that the mechanism of extremely low-volatility organic compounds (ELVOCs) formation is driven by RO2 autoxidation. The RO2 autoxidation pathway mainly includes the intramolecular hydrogen shift and the sequential O2 addition steps (Rissanen, et al., 2014). Compared with the RO2 autoxidation pathways, oligomerization reactions involving CIs as the repeat units, preserve carbon oxidation state and increase the number of a carbon backbone moiety, and therefore lead to a large reduction in the volatility (Wang, et al., 2016). Moreover, oligomerization reaction proceed over a shorter period of time during the early stage of biogenic SOA formation and growth (Heaton et al., 2007). Therefore, it is essential to investigate the gas phase Criegee chemistry-based mechanism of SOA formation and growth. Corresponding descriptions have been added in the page 5 line 116-127 and page 6 line 128-132 of the revised manuscript: On the other hand, Ehn et al. (2014) reported a large source of low-volatility SOA generated from the ozonolysis of

α-pinene and other endocyclic monoterpenes under atmospheric conditions, and proposed that the mechanism of extremely low-volatility organic compounds (ELVOCs) formation is driven by RO2 autoxidation. The RO2 autoxidation pathway mainly includes the intramolecular hydrogen shift and the sequential O2 addition steps (Rissanen et al., 2014). Also several groups obtained similar conclusions that the highly oxygenated molecules (HOM) are produced via RO2 autoxidation in the cyclohexene and terpenes ozonolysis systems (Kirkby et al., 2016; Berndt et al., 2018). Moreover, HOM are major contributors to aerosol particle formation and growth on a global scale (Tröstl et al., 2016; Stolzenburg et al., 2018). Compared with the RO2 autoxidation pathways, oligomerization reactions involving CIs as the repeat units, preserve carbon oxidation state and increase the number of a carbon backbone moiety, and therefore lead to a large reduction in the volatility (Wang et al., 2016). Moreover, oligomerization reaction proceeds over a shorter period of time during the early stage of biogenic SOA formation and growth (Heaton et al., 2007). Therefore, we think that it is essential to investigate the gas phase Criegee chemistry-based mechanism of SOA formation and growth. 5. All optimized geometries of the stationary points must be added to supplementary material. Pictures are not sufïiňĄcient, z-matrices must be included. Also The imaginary frequencies which are used in your Eckart calculations should be included. Response: Based on the Reviewer's suggestion, the optimized geometries, z-matrices and vibrational frequencies of all stationary points are added in the Figures S4, S6-S8, and the imaginary frequencies of all transition states in Eckart calculations are also added in the Figures S4, S6-S8 in the supplementary material. 6. Be very careful about referring to SOAs as individual aerosols. As this work may relate to new particle formation this may technically be correct, but this usage is often problematic. Line 26 has the INCORRECT usage, it should be "secondary organic aerosol (SOA)", because the general term refers to mass added to existing aerosol due to condensation of material onto existing particles. Response: Based on the Reviewer's suggestion, the secondary organic aerosols (SOA) has been corrected in the revised manuscript. 7. You state the importance of entropy in the free energy barriers, but you do not discuss

its origin. Please comment on key vibrational modes that contribute to entropic factors. Response: According to the principle of statistical thermodynamics, the entropy can be described as eqn (2) (2) where H is the enthalpy, G is the free energy, T is the temperature in Kelvin. The relationship between the entropy and the partition function can be written as eqn (3) (3) where k is the Boltzmann constant, q is the partition function, it mainly includes translation (qtrans), vibration (qvib), external rotation (qrot), electronic (qele) and torsional (qtor) partition functions (q = qtransqvibqrotqeleqtor) (Mendes, et al., 2014). Among these partition functions, the qvib plays an important role in determining the entropic factors. Thus, the qvib is used to evaluate the contribution of vibrational mode to the entropic factors. The qvib is expressed as follows: (4) Table S2 lists the partition function of every vibrational mode involved in the complex IM1a. As shown in Table S2, the partition functions of low frequency vibrational mode (< 200 cm-1) are significantly higher than the high frequency vibrational mode (> 200 cm-1), and their contribution is up to 70.5 percent. The result implies that the low frequency vibrational mode contributes to entropic factor is significant. Similar conclusion is also obtained from the IM2a case (Table S3). Corresponding descriptions have been added in the page 11 line 293-299 of the revised manuscript: The partition function of every vibrational mode involved in the complex IM1a is listed in Table S2. As shown in Table S2, the partition function of low frequency vibrational mode (< 200 cm-1) is significantly higher than the high frequency vibrational mode (> 200 cm-1), and their contribution is up to 70.5 percent. The result implies that the low frequency vibrational mode contributes to entropic factor is significant. Similar conclusion is also obtained from the IM2a case (Table S3). Table S2 The partition function of every vibrational mode involved in the complex IM1a N ïĄő qvib percent(%) 1 51.49 4.03 30.43 2 123.66 1.66 12.52 3 149.16 1.37 10.31 4 158.76 1.28 9.66 5 199.39 1.00 7.58 6 242.53 0.81 6.12 7 257.19 0.76 5.74 8 422.78 0.42 3.15 9 501.75 0.33 2.48 10 538.04 0.30 2.24 11 642.00 0.22 1.69 12 723.92 0.18 1.37 13 858.58 0.13 0.97 14 896.89 0.12 0.89 15 958.09 0.10 0.76 16 1070.70 0.08 0.58 17 1093.27 0.07 0.55 18 1112.93 0.07 0.52 19 1134.12 0.07 0.50 20 1270.31 0.05 0.36 21 1300.08 0.04 0.33 22 1397.45 0.03 0.26

23 1429.61 0.03 0.24 24 1456.77 0.03 0.23 25 1506.87 0.03 0.20 26 1588.46 0.02 0.17 27 1674.72 0.02 0.13 28 3088.99 0.00 0.00 29 3148.98 0.00 0.00 30 3162.08 0.00 0.00 31 3162.65 0.00 0.00 32 3305.08 0.00 0.00 33 3868.49 0.00 0.00 Table S3 The partition function of every vibrational mode involved in the complex IM2a N ïĄő qvib percent(%) 1 45.57 4.56 19.74 2 66.77 3.10 13.44 3 93.88 2.20 9.52 4 102.82 2.00 8.68 5 122.46 1.67 7.25 6 144.25 1.41 6.12 7 151.51 1.34 5.82 8 186.88 1.08 4.66 9 236.15 0.84 3.62 10 242.41 0.81 3.52 11 324.58 0.58 2.51 12 383.38 0.47 2.05 13 460.65 0.37 1.61 14 475.56 0.35 1.54 15 546.86 0.29 1.25 16 589.00 0.26 1.12 17 676.46 0.20 0.89 18 704.48 0.19 0.82 19 751.93 0.17 0.73 20 889.93 0.12 0.52 21 904.59 0.12 0.50 22 957.33 0.10 0.44 23 1053.66 0.08 0.35 24 1082.87 0.07 0.33 25 1103.67 0.07 0.31 26 1123.39 0.07 0.29 27 1129.87 0.07 0.29 28 1139.95 0.06 0.28 29 1188.07 0.06 0.25 30 1271.30 0.05 0.20 31 1306.97 0.04 0.19 32 1353.81 0.04 0.17 33 1383.99 0.04 0.16 34 1415.10 0.03 0.14 35 1438.67 0.03 0.14 36 1455.62 0.03 0.13 37 1457.70 0.03 0.13 38 1501.08 0.03 0.12 39 1569.37 0.02 0.10 40 1663.59 0.02 0.08 41 3104.57 0.00 0.00 42 3113.88 0.00 0.00 43 3140.47 0.00 0.00 44 3173.49 0.00 0.00 45 3187.95 0.00 0.00 46 3286.9 0.00 0.00 47 3436.06 0.00 0.00 48 3910.66 0.00 0.00 8. Did the authors look for cyclic products? For example products where both dashed bonds in IM1a becoming full covalent bonds? Response: All the pre-reactive complexes and products involved in the title reaction system are the cyclic structures. For example, the bimolecular reaction of CH2OO with HO-CH2OO-H (Pa1) begins with the barrierless formation of pre-reactive complexes IM1a and IM1b held together by weak hydrogen bonds and vdW forces. Then, the -OOH and -OH fragments in Pa1 immediately add to the CH2OO central carbon atom to produce P1a and P1b. The detailed reaction mechanism mainly includes that the -O3(-O1) fragment of Pa1 moves to approach the CH2OO central carbon atom, whereas the -H4(-H3) atom gets attached to the terminal oxygen atom leading to products P1a and P1b (see Table S4). In the revised manuscript, atoms in molecules (AIM) analysis at the bond critical point (BCP) for the forming bonds (B1(O5-H4), B2(O3-C4), B3(O5-H3) and B1(O1-C4)) is performed with M06-2X functional (Biegler et al., 2000). The electronic density (),

Laplacian (ïČŚ2), and the three eigenvalues of the Hessian of BCP are listed in Table S4. As shown in Table S4, the ïČŚ2 values of all forming bonds are negative, indicating that they are covalent bonds. The values of B1 and B3 are significantly higher than that of the B2 and B4, showing that the bond strength of the former case is higher than the latter case. Corresponding descriptions have been added in the page 12 line 320-326 of the revised manuscript: The electronic density (), Laplacian (ïČŚ2), and the three eigenvalues of the Hessian of the complexes IM1a and IM1b are displayed in Table S4. As shown in Table S4, the ïČŚ2 values of all forming bonds (B1(O5-H4), B2(O3-C4), B3(O5-H3) and B1(O1-C4)) are negative, indicating that they are covalent bonds. The values of B1 and B3 are significantly higher than that of the B2 and B4, showing that the bond strength of the former case is higher than the latter case.

Table S4 AIM properties at the bond critical points for the forming bonds B1-B4 Bond (e/Å3) ïČŚ2(e/Å3) Eigenvalue 1 Eigenvalue 2 Eigenvalue 3 B1(O5-H4) 0.370 -2.776 -1.9316 -1.8598 1.0148 B2(O3-C4) 0.271 -0.559 -0.5734 -0.5112 0.5258 B3(O5-H3) 0.364 -2.760 -1.945 -1.8743 1.0588 B4(O1-C4) 0.269 -0.565 -0.5734 -0.5054 0.5139 9. Do you rely solely on free energy estimate outputs? Are other methods such as SCTST too costly? Response: The rate coefficients of elementary reactions are calculated using a combination of canonical transition state theory (CTST) and an asymmetric Eckart tunneling correction based on the free energies obtained from the M06-2X method, in the temperature range from 273 to 400 K. The predicted free energies are equal to the thermal correction to Gibbs free energies at the M06-2X/6-311+G(2df,2p) level plus the electronic energies obtained at the M06-2X/def2-TZVP level. In order to assess the reliability of our kinetics study, the rate coefficients of HO-CH2OO-H (Pa1) + CH2OO (R1a) and HO-CH2OO-H (Pa1) + anti-CH3CHOO (R9) reactions are recomputed employing the canonical variational transition state theory (CVTST) with Eckart tunneling correction. The calculated result is listed in Table S9. As shown in Table S9, the predicted rate coefficients kCTST(R1a) and kCVTST(R1a) decrease with increasing temperature, and they exhibit a negative temperature dependence. The difference between kCTST(R1a) and

kCVTST(R1a) decreases in the range of 2.3 (273 K) to 1.8 (400 K). Such discrepancy between CTST and CVTST ones is acceptable. Similar conclusion is also obtained from the rate coefficients between kCTST(R9) and kCVTST(R9). It is concluded that the CTST/Eckart method allows one to reliably describe the kinetics parameters. Corresponding descriptions have been added in the page 18 line 506 and page 19 line 507-514 of the revised manuscript: In order to assess the reliability of our kinetics study, the rate coefficients of some selected reactions R1a and R9 are recomputed employing the canonical variational transition state theory (CVTST) with Eckart tunneling correction. The calculated result is listed in Table S9. As shown in Table S9, the difference between kCTST(R1a) and kCVTST(R1a) decreases in the range of 2.3 (273 K) to 1.8 (400 K). Such rate coefficients discrepancy between CTST and CVTST ones is acceptable. Similar conclusion is also obtained from the rate coefficients between kCTST(R9) and kCVTST(R9). It is concluded that the CTST/Eckart method allows one to reliably describe the kinetics parameters. Table S9 Rate coefficients (cm3 molecule-1 s-1) of elementary reactions R1a and R9 computed T kCTST(R1a) kCVTST(R1a) kCTST(R9) kCVTST(R9) 273 1.2 × 10-11 3.5 × 10-11 5.5 × 10-9 1.3 × 10-8 280 9.4 × 10-12 2.6 × 10-11 3.7 × 10-9 8.5 × 10-9 298 5.4 × 10-12 1.4 × 10-11 1.5 × 10-9 3.2 × 10-9 300 5.1 × 10-12 1.3 × 10-11 1.3 × 10-9 2.9 × 10-9 320 3.0 × 10-12 7.2 × 10-12 5.5 × 10-10 1.1 × 10-9 340 1.9 × 10-12 4.2 × 10-12 2.6 × 10-10 5.0 × 10-10 360 1.2 × 10-12 2.7 × 10-12 1.4 × 10-10 2.4 × 10-10 380 8.6 × 10-13 1.8 × 10-12 7.1 × 10-11 1.3 × 10-10 400 6.3 × 10-13 1.2 × 10-12 4.1 × 10-11 7.3 × 10-11 10. In sections 3.3 and 3.4, the discussion of loss processes for CI is ïňĆawed. Unimolecular decay is always a signiïňĄcant loss process. You seem to misinterpret the references you cite, both Drozd et al. and Long et al. find short thermal lifetimes for the CI formed in ozonolysis.(3,4) The authors must revise their statements to make clear that CI generally have signiïňĄcant unimolecular decay. Response: Long et al. (2016) proposed that the predominant pathway of unimolecular decay of syn-CH3CHOO is isomerization to vinyl hydroperoxide (VHP) via the hydrogen atom migration from the methyl group to the terminal oxygen atom, then the

decomposition of VHP produces OH radical. Also Donahue et al. (2011) obtained similar conclusion that syn-CI isomerization to VHP is preferable due to the low ring strain of H-atom transfer transition state. Both the prompt and thermal unimolecular decay of the energized VHP may dissociate to OH radical, and their yields are strongly pressure and temperature dependents (Kroll, et al., 2001a,b). The preferable route of unimolecular decay of anti-CH3CHOO is ring-closure to dioxirane via an oxygen atom transfer (Donahue et al, 2011; Taatjes et al., 2013; Long et al., 2016). The dioxirane can finally isomerize to acetic acid via the “hot acid” channel (Kroll, et al., 2001a). Alternatively, the syn- and anti-CH3CHOO may undergo bimolecular reactions with water vapor lead to the formation of HO-C(CH3)HOO-H (Anglada et al., 2011). Long et al. (2018) proposed that the unimolecular decay of (CH3)2COO is the predominant pathway above 240 K, whereas it can compete with the reaction (CH3)2COO + SO2 below 240 K. Drozd et al. (2017) elucidated that tunneling for both the thermal and prompt unimolecular decay of (CH3)2COO is significant. Also Lester et al. (2018) obtained similar conclusion in the unimolecular decay of (CH3)2COO to OH radical reaction that the contribution of tunneling to the unimolecular decay rates is significant. Alternatively, the (CH3)2COO may react with water vapour leading to the formation of HO-C(CH3)2OO-H (Anglada et al., 2016). Corresponding descriptions have been added in the page 14 line 380-389, page 15 line 390-393 and page 16 line 437-445 of the revised manuscript: Long et al. (2016) proposed that the predominant pathway of unimolecular decay of syn-CH3CHOO is isomerization to vinyl hydroperoxide (VHP) via the hydrogen atom migration from the methyl group to the terminal oxygen atom, then the decomposition of VHP produces OH radical. Also Donahue et al. (2011) obtained similar conclusion that syn-CI isomerization to VHP is preferable due to the low ring strain of H-atom transfer transition state. Both of the prompt and thermal unimolecular decay of the energized VHP may dissociate to OH radical, and their yields are strongly pressure and temperature dependents (Kroll et al., 2001a,b). The preferable route of unimolecular decay of anti-CH3CHOO is ring-closure to dioxirane via an oxygen atom transfer (Donahue et al., 2011; Taatjes et al., 2013;

Long et al., 2016). The dioxirane can finally isomerize to acetic acid via the “hot acid” channel (Kroll et al., 2011b). Alternatively, the syn- and anti-CH3CHOO may undergo bimolecular reactions with water vapor lead to the formation of HO-C(CH3)HOO-H (Anglada et al., 2011). Long et al. (2018) proposed that the unimolecular decay of (CH3)2COO is the predominant pathway above 240 K, whereas it can compete with the reaction (CH3)2COO + SO2 below 240 K. Drozd et al. (2017) elucidated that tunneling for both the thermal and prompt unimolecular decay of (CH3)2COO is significant. Also Lester et al. (2018) obtained similar conclusion in the unimolecular decay of (CH3)2COO to OH radical reaction that the contribution of tunneling to the unimolecular decay rates is significant. Alternatively, the (CH3)2COO may react with water vapour leading to the formation of HO-C(CH3)2OO-H (Anglada et al., 2016). 11. The energy labels in the supplement are confusing. The italics/non-italics energies are not always in same vertical order. Change the ïňĄgure labels to make the non-italics energy the upper number in all cases. Do this for the main manuscript ïňĄgures as well. Response: Based on the Reviewer’s suggestion, the non-italics energies have been placed in the upper number in the manuscript and supplement figures. 12. There are a number of awkward sentences/phrases, missing words, or grammatically confusing sentences. Carefully check over this document. I have listed a number of these below. Line 27 change to “inïňĆuence” Line 43 Add Guenther et al as a reference for alkene emissions.5 Line 119 change to “is the dominant..” 132 change to “reactions occur during the. . .” 147 change to “there is little known of the reactivity. . .” 167 change to “represents” 168 change to “needs” 238 change to “possess OH and OOH” 246 change to “particularly” 267 - It is confusing to see a negative energy of stability, re-word this, and other in- stances, to be clearer. 315-317 You have an error the citations to Kroll et al. The year should be 2001.(6,7) Response: Based on the Reviewer’s suggestion, the sentences/phrases, missing words, and the grammatically confusing sentences have been corrected carefully in the revised manuscript. âĂČ References Anglada, J. M., and Solé, A.: Impact of water dimer on the atmospheric reactivity of carbonyl oxides, Phys. Chem. Chem.

Phys., 18, 17698-17712, 10.1039/c6cp02531e, 2016. Anglada, J. M., González, J., and Torrent-Sucarrat, M.: Effects of the substituents on the reactivity of carbonyl oxides. A theoretical study on the reaction of substituted carbonyl oxides with water, Phys. Chem. Chem. Phys., 13, 13034-13045, 10.1039/c1cp20872a, 2011. Biegler, F. J., Derdau, R., Bayles, D., and Bader, R. F. W.: AIM2000, Version 1, 2000. Chao, W., Hsieh, J. T., Chang, C. H., and Lin, J. J. M.: Direct kinetic measurement of the reaction of the simplest Criegee intermediate with water vapor, Science, 347, 751-4, 10.1126/science.1261549, 2015. Donahue, N. M., Drozd, G. T., Epstein, S. A., Presto, A. A., and Kroll, J. H.: Adventures in ozoneland: down the rabbit-hole, Phys. Chem. Chem. Phys., 13, 10848-10857, 10.1039/c0cp02564j, 2011. Drozd, G. T., Kurtén, T., Donahue, N. M., and Lester, M. I.: Unimolecular decay of the dimethyl-substituted Criegee intermediate in alkene ozonolysis: decay time scales and the importance of tunneling, J. Phys. Chem. A, 121, 6036-6045, 10.1021/acs.jpca.7b05495, 2017. Ehn, M., Thornton, J. A., Kleist, E., Sipilä, M., Junninen, H., Pullinen, I., Springer, M., Rubach, F., Tillmann, R., Lee, B., Lopez-Hilfiker, F., Andres, S., Acir, I. H., Rissanen, M., Jokinen,T., Schobesberger, S., Kangasluoma, J., Kontkanen, J., Nieminen, T., Kurtén, T., Nielsen, L. B., Jørgensen, S., Kjaergaard, H. G., Canagaratna, M., Maso, M. D., Berndt, T., Petäjä, T., Wahner, A., Kerminen, V. M., Kulmala, M., Worsnop, D. R., Wildt, J., and Mentel T. F.: A large source of low-volatility secondary organic aerosol, Nature, 506, 476-9, 10.1038/nature13032, 2014. Heaton, K. J., Dreyfus, M. A., Wang, S., and Johnston, M. V.: Oligomers in the early stage of biogenic secondary organic aerosol formation and growth, Environ. Sci. Technol., 41, 6129-6136, 10.1021/es070314n, 2007. Kroll, J. H., Clarke, J. S., Donahue, N. M., and Anderson, J. G.: Mechanism of HOx formation in the gas-phase ozone-alkene reaction. 1. direct, pressure-dependent measurements of prompt OH yields, J. Phys. Chem. A, 105, 1554-1560, 10.1021/jp002121r, 2001. Kroll, J. H., Hanisco, T. F., Donahue, N. M., Demerjian, K. L., and Anderson, J. G.: Accurate, direct measurements of OH yields from gas-phase ozone-alkene reactions using an in situ LIF instrument, Geophys. Res. Lett., 28, 3863-3866, 10.1029/2001GL013406, 2001. Kumar, M.,

Busch, D. H., Subramaniam, B., and Thompson, W. H.: Role of tunable acid catalysis in decomposition of α-hydroxyalkyl hydroperoxides and mechanistic implications for tropospheric chemistry, J. Phys. Chem. A, 118, 9701-9711, 10.1021/jp505100x, 2014. Lester, M. I., and Klippenstein, S. J.: Unimolecular decay of Criegee intermediates to OH radical products: prompt and thermal decay processes, Acc. Chem. Res., 51, 978-985, 10.1021/acs.accounts.8b00077, 2018. Lin, L. C., Chang, H. T., Chang, C. H., Chao, W., Smith, M. C., Chang, C. H., Lin, J. J. M., and Takahashi, K.: Competition between H2O and (H2O)2 reactions with CH2OO/CH3CHOO, Phys. Chem. Chem. Phys., 18, 4557-4568, 10.1039/C5CP06446E, 2016. Long, B., Bao, J. L., and Truhlar, D. G.: Atmospheric chemistry of Criegee intermediates: unimolecular reactions and reactions with water, J. Am. Chem. Soc., 138, 14409-14422, 10.1021/jacs.6b08655, 2016. Long, B., Bao, J. L., and Truhlar, D. G.: Unimolecular reaction of acetone oxide and its reaction with water in the atmosphere, Proc. Natl. Acad. Sci. U.S.A., 115, 6135-6140, 10.1073/pnas.1804453115, 2018. Mendes, J., Zhou, C. W., and Curran, H. J.: Theoretical chemical kinetic study of the H-atom abstraction reactions from aldehydes and acids by H atoms and OH, HO2, and CH3 radicals, J. Phys. Chem. A, 118, 12089-12104, 10.1021/jp5072814, 2014. Novelli, A., Hens, K., Ernest, C. T., Martinez, M., Nölscher, A. C., Sinha, V., Paasonen, P., Petäjä, T., Sipilä, M., Elste, T., Plass-Dülmer, C., Phillips, G. J., Kubistin, D., Williams, J., Vereecken, L., Lelieveld, J., and Harder, H.: Identifying Criegee intermediates as potential oxidants in the troposphere, Atmos. Chem. Phys. Discuss., 10.5194/acp-2016-919, 2016. Novelli, A., Hens, K., Ernest, C. T., Martinez, M., Nölscher, A. C., Sinha, V., Paasonen, P., Petäjä, T., Sipilä, M., Elste, T., Plass-Dülmer, C., Phillips, G. J., Kubistin, D., Williams, J., Vereecken, L., Lelieveld, J., and Harder, H.: Estimating the atmospheric concentration of Criegee intermediates and their possible interference in a FAGE-LIF instrument, Atmos. Chem. Phys., 17, 7807-7826, 10.5194/acp-17-7807-2017, 2017. Rissanen, M. P., Kurtén,T., Sipila, M., Thornton, J. A., Kangasluoma, J., Sarnela, N., Junninen, H., Jørgensen, S., Schallhart, S., Kajos, M. K., Taipale, R., Springer, M., Mentel, T. F., Ruuskanen, T., Petäjä, T., Worsnop, D. R., Kjaergaard, H. G., and Ehn M.: The for-

mation of highly oxidized multifunctional products in the ozonolysis of cyclohexene, J. Am. Chem. Soc., 136, 15596-15606, 10.1021/ja507146s, 2014. Smith, M. C., Chang, C. H., , W., Lin, L. C., Takahashi, K., Boering, K. A., and Lin, J. J. M.: Strong negative temperature dependence of the simplest Criegee intermediate CH2OO reaction with water dimer, J. Phys. Chem. Lett., 6, 2708-2713, 10.1021/acs.jpclett.5b01109, 2015. Taatjes, C. A., Welz, O., Eskola, A. J., Savee, J. D., Scheer, A. M., Shallcross, D. E., Rotavera, B., Lee, E. P. F., Dyke, J. M., Mok, D. K. W., Osborn, D. L., and Percival, C. J.: Direct measurements of conformer-dependent reactivity of the Criegee intermediate CH3CHOO, Science, 340, 177-180, 10.1126/science.1234689, 2013. Wang, M., Yao, L., Zheng, J., Wang, X., Chen, J., Yang, X., Worsnop, D. R., Donahue, N. M., and Wang, L.: Reactions of atmospheric particulate stabilized Criegee intermediates lead to high-molecular-weight aerosol components, Environ. Sci. Technol., 10.1021/acs.est.6b02114, 50, 5702-5710, 2016.

Please also note the supplement to this comment:
https://www.atmos-chem-phys-discuss.net/acp-2018-935/acp-2018-935-AC1-supplement.pdf

---

Interactive comment on Atmos. Chem. Phys. Discuss., https://doi.org/10.5194/acp-2018-935, 2018.

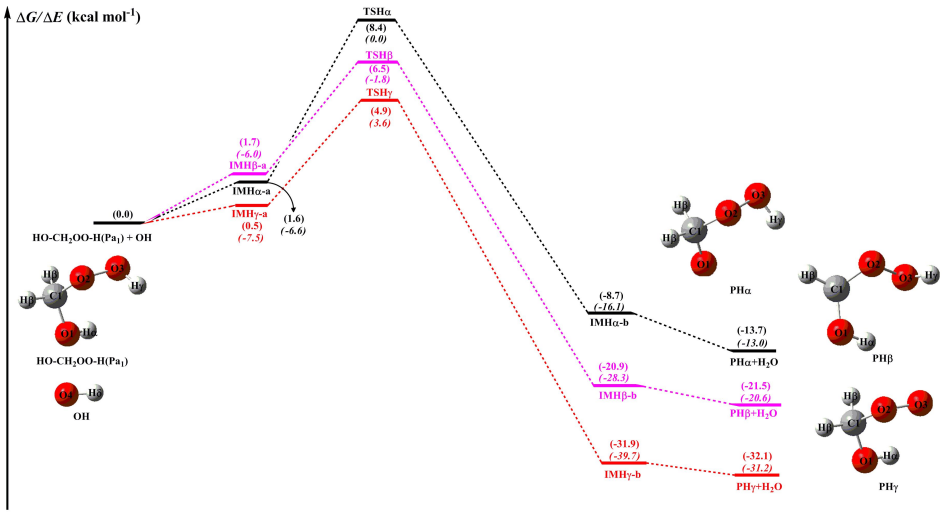
ΔG/ΔE (kcal mol-1)
TSHα
(8.4)
(0.0)
TSHβ
(6.5)
(-1.8)
TSHγ
(4.9)
(3.6)
(1.7)
(-6.0)
IMHβ-a
IMHα-a
IMHγ-a
(0.5)
(-7.5)
(0.0)
HO-CH2OO-H(Pa1) + OH
(1.6)
(-6.6)
HO-CH2OO-H(Pa1)
OH
(-8.7)
(-16.1)
IMHα-b
(-13.7)
(-13.0)
PHα+H2O
(-20.9)
(-28.3)
IMHβ-b
(-21.5)
(-20.6)
PHβ+H2O
(-31.9)
(-39.7)
IMHγ-b
(-32.1)
(-31.2)
PHγ+H2O
PHα
PHβ
PHγ

Fig. 1.